

RESEARCH

Open Access



SCR-6852, an oral and highly brain-penetrating estrogen receptor degrader (SERD), effectively shrinks tumors both in intracranial and subcutaneous ER + breast cancer models

Feng Zhou^{1,2†}, Guimei Yang^{2†}, Liting Xue^{1,2†}, Yajing Liu², Yao Guo², Ji Zhu², Linlin Yuan², Peng Gu³, Feng Tang^{1,3}, Jinwen Shan² and Renhong Tang^{1,2,3*†}

Abstract

Background Targeted estrogen receptor degradation has been approved to effectively treat ER + breast cancers. Due to the poor bioavailability of fulvestrant, the first generation of SERD, many efforts were made to develop oral SERDs. With the approval of Elacestrant, oral SERDs demonstrated superior efficacy than fulvestrant. However, due to the poor ability of known SERDs to penetrate the blood–brain barrier (BBB), breast cancer patients with brain metastasis cannot benefit from clinical SERDs.

Methods The ER inhibitory effects were evaluated on ER α protein degradation, and target genes downregulation. And anti-proliferation activities were further determined in a panel of ER+ breast cancer cell lines. The subcutaneous and intracranial ER+ tumor models were used to evaluate the efficacy of anti-tumor effects. Brain penetrability was determined in multiple animal species.

Results SCR-6852 is a novel SERD and currently is under early clinical evaluation. In vitro studies demonstrated that it strongly induced both wildtype and mutant ER α degradation. It potently inhibited cell proliferation in a panel of ER+ breast cancer cell lines, including the cell lines containing *ESR1* mutations (Y537 and D538). Furthermore, SCR-6852 exhibited pure antagonistic activities on the ER α signal axis identified both in vitro and in vivo. Oral administration of SCR-6852 at 10 mg/kg resulted in tumor shrinkage which was superior to Fulvestrant at 250 mg/kg, notably, in the intracranial tumor model, SCR-6852 effectively inhibited tumor growth and significantly prolonged mice survival, which correlated well with the high exposure in brains. In addition to mice, SCR-6852 also exhibited high brain penetrability in rats and dogs.

[†]Feng Zhou, Guimei Yang and Liting Xue have contributed equally to this work.

[†]Renhong Tang jointly supervised this work.

*Correspondence:

Renhong Tang

renhong.tang@simceregroup.com

Full list of author information is available at the end of the article



© The Author(s) 2023. **Open Access** This article is licensed under a Creative Commons Attribution 4.0 International License, which permits use, sharing, adaptation, distribution and reproduction in any medium or format, as long as you give appropriate credit to the original author(s) and the source, provide a link to the Creative Commons licence, and indicate if changes were made. The images or other third party material in this article are included in the article's Creative Commons licence, unless indicated otherwise in a credit line to the material. If material is not included in the article's Creative Commons licence and your intended use is not permitted by statutory regulation or exceeds the permitted use, you will need to obtain permission directly from the copyright holder. To view a copy of this licence, visit <http://creativecommons.org/licenses/by/4.0/>. The Creative Commons Public Domain Dedication waiver (<http://creativecommons.org/publicdomain/zero/1.0/>) applies to the data made available in this article, unless otherwise stated in a credit line to the data.

Conclusions SCR-6852 is a novel SERD with high potency in inducing ER α protein degradation and pure antagonistic activity on ER α signaling in vitro and in vivo. Due to the high brain penetrability, SCR-6852 could be used to treat breast patients with brain metastasis.

Keywords SCR-6852, SERD, Fulvestrant, Estrogen receptor, Breast cancer, Breast cancer brain metastasis

Background

Breast cancer (BC) is the most common malignancy in women around the world, and the overall rates of BC incidence and mortality for the world population have continuously increased [1, 2]. According to the GLOBOCAN 2020 estimation by the International Agency for Research on Cancer, female breast cancer had surpassed lung cancer as the most commonly diagnosed cancer, with an estimated 2.3 million new cases per year [3]. Approximately 80% of breast cancers are estrogen receptor-positive (ER+) which results in the most breast cancer deaths [4, 5]. Despite substantial improvements achieved both in disease-free survival and overall survival with endocrine therapies in early-stage breast cancers [6], up to 30% of patients diagnosed with operable ER+ tumors eventually metastasized [7].

Estrogen receptor has been targeted for breast cancer treatment for over a century [8, 9]. Endocrine therapy is the main therapeutic choice in clinical practices for ER-positive metastatic breast cancer (mBC) patients with proven clinical benefits [10]. Tamoxifen, the first ER modulator has reduced breast cancer recurrence and annual mortality rate by 50% and 31%, respectively, since the approval by the Food and Drug Administration (FDA) for the treatment of women with advanced breast cancer [11]. However, numerous studies demonstrated that tamoxifen is a partial ER agonist with both additive and antagonistic effects to estradiol [12]. Furthermore, some resistant mutations (e.g. Y537S and D538G) are observed in the ER ligand-binding domain (LBD) after the long-term treatment of tamoxifen, which leads to the disease progression [13]. Estrogen receptor degrader/down-regulator works as a pure ER antagonist that acts by binding to ER and consequently induces the rapid degradation of ER [8, 14]. Fulvestrant is the first SERD available in clinical practice [15] and the efficacies were well demonstrated by extensive clinical trials. In a second-line setting trial, Fulvestrant was still proved to be effective in patients having experienced progression after previous endocrine therapy with tamoxifen, with clinical benefits both in PFS (6.5 vs. 5.5 months; $p=0.05$) and OS (26.4 months with Fulvestrant HD 500 mg and 22.3 months with 250 mg dose regimen $p=0.05$) [16]. Clinical investigation revealed that side effects associated with tamoxifen was

not observed in Fulvestrant either in monotherapy or in combination with other agents, for the treatment of ER-positive advanced breast cancer [17, 18]. However, poor bioavailability, slow action associated with intramuscular injection, and low response, these limitations of Fulvestrant have driven a critical need to develop a clinically proven, orally bioavailable SERD. At present, a few numbers of new generated oral SERDs were developed including Elacestrant (RAD-1901) which was recently approved for medical use in the United States [19], GDC-9545 (Roche) and AZD9833 (AstraZeneca). The last two oral SERDs also demonstrated promising antitumor activity in patients with advanced ER-positive breast cancer in phase 2 trials [20–22].

Breast cancer brain metastasis (BCBM) is the second most common cause of brain metastasis, and its occurrence has been rising in the past two decades with significant improvement in the survival of advanced breast cancer patients [23]. The current treatment options for ER-positive breast cancer patients with brain metastases are limited, including surgical resection and local radiotherapy. However, not all patients are suitable for those treatments. And patients with brain metastases who receive these treatments eventually develop refractoriness in a short time. Medicines with high BBB penetration capability could be a better choice for those brain metastasis patients. However, although several SERDs were investigated in the clinic, few SERDs were reported with brain penetration character and had been investigated in brain MBC patients, with the exception of OP-1250 from Olema Oncology. Thus, the development of an oral SERD with high BBB penetrability is still an unmet medical need. SCR-6852 is an oral, highly BBB penetrable and selective ER α degrader which is under clinical evaluation. Preclinical data showed that SCR-6852 strongly inhibited the growth of ER-positive breast cancer cells by inducing ER α degradation and following the complete inhibition of ER target genes transcription. In ER+ subcutaneous tumors, SCR-6852 demonstrated superior anti-tumor activities than Fulvestrant. Notably, SCR-6852 possessed high BBB penetrability in multiple pre-clinical animals and significantly promotes mouse survival in an intracranial tumor model. A combination of SCR-6852 and a CDK4/6 inhibitor revealed synergistically anti-tumor activities both in vitro and in vivo.

Methods

Cell lines

MCF-7 (#HTB-22), CAMA-1 (#HTB-21), HCC1500 (#CRL-2329), BT-474 (#HTB-20), and SK-BR-3 (#HTB-30) cells were purchased from ATCC. Especially, MCF-7 (#86012803) used in subcutaneous xenograft mouse model was purchased from ECACC. EFM-19 (#CBP60363) was from Cobiaer Bioscience. T47D (#KC-0199) was from KYinno Biotechnology. All cell authentication was conducted through short tandem repeat (STR) DNA profiling by Biowing and the routine screening for mycoplasma contamination was done using Lonza Mycoalert and Stratagene Mycosensor. Unless otherwise indicated, tissue culture supplements and medium were purchased from Hyclone, Corning, or Invitrogen. Cells were maintained as recommended by the vendor. MCF-7 was maintained in DMEM with 10% FBS, 0.01 mg/ml of Human insulin (Yeasen), and 1% NEAA. CAMA-1 was maintained in EMEM with 10% FBS. HCC1500 and EFM-19 were maintained in RPMI-1640 with 10% FBS. T47D was maintained in RPMI-1640 with 10% HI-FBS and 2 units/mL bovine insulin (Solarbio). BT-474 was maintained in Hybri-Care Medium (ATCC) with 1.5 g/L sodium bicarbonate and 10%FBS. SK-BR-3 was maintained in McCoy's 5A Medium with 10% FBS. MCF7 cells expressing the ER. Y537S variant (#CBP60380DR-3) was from Cobiaer Bioscience and maintained in MEM with 10%FBS containing 1%NEAA and 1 mM NaP. The MCF7 cells harbo D538G variant (WUXI_MCF7_ER_D538G_KI) were provided by Wuxi AppTec was cultured in EMEM with 10% FBS and 1% NEAA.

Compounds

SCR-6139, SCR-6515, and SCR-6852 were synthesized as described in (WO2021228210), GDC-9545 was synthesized described in (WO2019245974) (Compound A). AZD9833 was made as described in WO2018077630 (example 17), AZD9496 was purchased from Selleck (#S8372). ARV-471 was synthesized as described in WO2022132652 (compound 1c). Fulvestrant, 4-OH-tamoxifen, Palbociclib, Alpelisib and Elacestrant (RAD1901) were purchased from MCE.

Animals

All experimental procedures involving animals and their care were conducted in conformity with the State Council Regulations for Laboratory Animal Management (Enacted in 1988) and were approved by the Institutional Animal Care and Use Committee of the WuXi AppTec and Simcere, People's Republic of China. Female Balb/c nude mice at 6–8 weeks of age were purchased from Shanghai Lingchang Biotechnology Co., Ltd. (Shanghai, China). Female NOD.Cg-Prkdc^{scid} Il2rg^{tm1Vst}/Vst (NPG)

mice at 6–8 weeks of age were purchased from Beijing Vitalstar Biotechnology Co., Ltd. (Beijing, China). Female Sprague–Dawley (SD) rats at 3 weeks of age were purchased from Charles River (Beijing, China).

Molecular docking and molecular dynamic simulation

Molecular docking. The protein data bank (www.rcsb.org, PDB: 6ZOQ, resolution: 2.34) was used to derive the crystal structure of the human estrogen receptor alpha (ER α) protein. The downloaded protein was generated in the docking software MOE. The QuickPrep module of Molecular Operating Environment (MOE) 2022 is used to process the protein comprised by applying gas tier charges through the MMFF94x forcefield, adding hydrogen atoms, removing water molecules, 3D protonation of the structure, and minimizing the protein structure to a chosen gradient. Meanwhile, the WASH module and Energy Minimize of MOE were used for hydrogenation and energy minimization of small molecules.

After protein preparation and ligands preparation, 4-hydroxytamoxifen, Fulvestrant, SCR6139, and SCR6515 were docked with ER α . The active site was selected using rectangular coordinates based on the co-crystal ligand QNE. The docking algorithm was configured to use the triangle matcher placement approach [24], and the default GBVI/WSA dG technique was used as a docking function in MOE [25]. The binding poses of the compound with the highest five docking scores can be visualized in MOE. Finally, the most suitable pose was picked for the study.

Proliferation assays

Trypsinized cells were dispensed into 384-well plates in culture media and after overnight incubation cells were treated with compounds for 7 days. Cell viability was assessed using CellTiter-Glo (Promega) according to the manufacturer's protocol and relative luminescence units (RLU) were measured using an Envision Multilabel Reader (Perkin Elmer). Inhibition% was normalized to untreated samples and Fulvestrant treated samples or media samples. IC₅₀ and Imax were analyzed with IDBS XLfit.

In-cell Western assay

MCF-7 wild type and Y537S mutant cells were seeded at a density of 5000 cells per well into flat clear bottom tissue cultured-treated 384-well plates (Greiner) in culture media and after overnight incubation cells were treated with compounds for 24 h. Then plates were fixed with 4% formaldehyde, permeabilized with ice-cold methanol, and blocked with Odyssey Blocking Buffer (LI-COR). The fixed cells were incubated with rabbit anti- ER α antibody (CST#8644S) and mouse anti-GAPDH antibody

(Abcam #ab8245), washed and stained with IRDye 800 Goat anti-Rabbit IgG (Licor#926-32211) and IRDye 680 Goat anti-Mouse IgG (Licor#926-68070). ER α levels were quantitated using Sapphire RGBNIR (Azure), the acumen eX3 imaging system. Inhibition% was normalized to untreated samples and Fulvestrant-treated samples. IC₅₀ and Emax were analyzed with IDBS XLfit.

EFM-19, CAMA-1, HCC1500, T47D, and BT-474 were seeded into flat clear bottom tissue cultured-treated 96-well plates (Greiner) in culture media and after overnight incubation cells were treated with 100 nM compounds for 24 h. Then plates were fixed with 4% formaldehyde, permeabilized with ice-cold methanol, and blocked with Odyssey Blocking Buffer. The fixed cells were incubated with rabbit anti-ER α antibody and mouse anti-GAPDH antibody, washed and stained with IRDye 800 Goat anti-Rabbit IgG and IRDye 680 Goat anti-Mouse IgG. ER α levels were quantitated using Sapphire RGBNIR. Inhibition% was normalized to untreated samples and Fulvestrant-treated samples.

Western blot

The cells of MCF-7 and MCF7 ESR1Y537S were seeded in 6 well plates for 24 h. Then compounds with different concentrations were added to cell plates. After 5 days, all cell samples were lysed with ice-cold RIPA buffer (Sigma) for 30 min. The lysate supernatant was centrifuged at 4 °C centrifuge at 10000 rpm for 10 min. Protein concentrations were determined with Pierce™ BCA Protein Assay Kit (Thermo Fisher Scientific). Each sample with equal total proteins was mixed with a loading buffer. Proteins from cell lysates were separated electrophoretically using NuPAGE 4–12% Bis-Tris Gels (Thermo Fisher Scientific) in MOPS buffer (Thermo Fisher Scientific). Gels were then electroblotted onto PVDF membranes (Bio-RAD). The blots were blocked with 5% BSA (Sigma) in TBST buffer for 1 h and then incubated with primary antibodies overnight at 4 °C. Blots were washed with TBST, incubated with secondary antibodies for 1 h, and washed with TBST. The blots were detected by SuperSignal™ West Dura Extended Duration Substrate (Thermo Fisher Scientific) and scanned using Sapphire RGBNIR (Azure). The protein levels were quantitated using ImageJ and normalized to β -Actin. Percent objective protein was defined as normalized treated sample/normalized untreated cells \times 100. Primary antibodies: Rabbit anti-ER α (D8H8) (1:3000, CST#8644S), Rabbit phospho-Rb (Ser807/811) (1:3000, #8516S), Mouse anti-Rb (4H1) (1:3000, CST# 9309S), Rabbit anti-cyclin D1(1:3000, Abcam#49604S), Rabbit anti- β -Actin (13E5) (1:5000, CST# 4970S). Secondary antibodies: Goat Anti-Mouse IgG H&L (HRP) (1:10000, Abcam#Ab6789), Goat Anti-Rabbit IgG H&L (HRP) (1:10000, Abcam#Ab205718).

Gene expression analysis by RNA-sequencing

MCF7 were cultured in hormone deprivation media (with 10% charcoal-stripped FBS) for at least 3 days before assay. Trypsinized cells were seeded in a 12-well plate, stimulated with 1 nM β -estradiol (E2), and treated with/without 1 μ M compounds for 24 h. Total RNA was extracted using the TRIzol reagent according to the manufacturer's protocol. RNA purity and quantification were evaluated using the NanoDrop 2000 spectrophotometer (Thermo Scientific, USA). RNA integrity was assessed using the Agilent 2100 Bioanalyzer (Agilent Technologies, Santa Clara, CA, USA). Then the libraries were constructed using TruSeq Stranded mRNA LT Sample Prep Kit (Illumina, San Diego, CA, USA) according to the manufacturer's instructions. The transcriptome sequencing and analysis were conducted by OE Biotech Co., Ltd. (Shanghai, China). The libraries were sequenced on an Illumina HiSeq X Ten platform and 150 bp paired-end reads were generated. About 48 ~ 50 M raw reads for each sample were generated. Raw data (raw reads) of FASTq format were firstly processed using Trimmomatic [26] and the low-quality reads were removed to obtain the clean reads. Then about 47 ~ 48 M clean reads for each sample were retained for subsequent analyses. The clean reads were mapped to the human genome (GRCh38) using HISAT2 [27]. FPKM [28] of each gene was calculated using Cufflinks [29], and the read counts of each gene were obtained by HTSeqcount [30]. Differential expression analysis was performed using the DESeq (2012) R package [6]. P value < 0.05 and foldchange > 2 or foldchange < 0.5 was set as the threshold for significantly differential expression.

ER pathway activity evaluation

HCC1500, T47D, and EFM-19 were cultured in hormone deprivation media with 10% charcoal-stripped FBS for at least 3 days before assay. Trypsinized cells were seeded in a 12-well plate, stimulated with 1 nM E2, and treated with/without 1 μ M compounds for 24 h. Total RNA was extracted using QIAGEN RNeasy Plus Mini Kit (Qiagen), according to the manufacturer's protocol. The concentration of RNA samples was determined using NanoDrop 8000 (Thermo Scientific). SYBR Green expression assay (Qiagen#204154) was used to quantify GREB1 (Forward primer: CTGCCCCAGAATGGTTTTTA; reverse primer: GGACTGCAGAGTCCA GAAGC), AGR3 (Forward primer: GCTTTGGGTCTC TGCCTCTTAC; reverse primer: TTGACAATCTC CAGGTGATGA) and the house-keeping genes actin (OriGene#HP204660). The relative quantities were determined using $\Delta\Delta$ threshold cycle ($\Delta\Delta$ Ct), according to the manufacturer's instructions (Applied Biosystems).

Cell cycle analysis

Trypsinized MCF-7 cells were seeded in a 24-well plate and treated with single or combined compounds for 40 h. Cells were collected and stained with 50 mg/mL propidium iodide (PI) solution in the presence of RNase (1 mg/mL) for 30 min on ice. The cells were then resuspended and analyzed with a FACS (BD Canto plus). At least 10,000 cells were counted for analysis.

MCF-7 and T47D subcutaneous xenograft mouse models

Female Balb/c nude mice were used for MCF-7 and T47D tumor subcutaneous xenograft studies. At least one day before tumor cell implantation, estrogen pellets (0.18 mg, 17 β -Estradiol, 60-day release, Innovative Research of America, Sarasota, FL, USA) were implanted subcutaneously. Each mouse was subcutaneously injected with 1×10^7 MCF-7 (ECACC) or T47D cells in the right flank, and tumor growth was monitored. The long diameter (a) and the short diameter (b) of the tumor were measured using a caliper, and the tumor volume was calculated using the following formula: $V = 0.5 \times a \times b^2$. When the average tumor volume reached 100–200 mm³ (designated as Day 0 of the study), the mice were randomly assigned to several groups of 8 animals each and treated with vehicle, Fulvestrant (250 mg/kg, subcutaneous injection, once a week), Palbociclib (40 mg/kg, oral gavage, daily), SCR-6852 (0.3, 1, 3, or 10 mg/kg, oral gavage, daily), or combinations as indicated in each figure. Tumor volumes were evaluated twice per week. Treatment tolerability was assessed by body weight measurements and frequent observation for clinical signs of treatment-related adverse effects.

The intracranial MCF-7 tumor model

Female NPG mice were used for the intracranial MCF-7 tumor model. Three days before tumor cell implantation, estrogen pellets (0.72 mg, 17 β -Estradiol, 60-day release, Innovative Research of America, Sarasota, FL, USA) were implanted subcutaneously. Each mouse was intracranially injected with 2×10^6 MCF-7 (ATCC) cells. Eight days after tumor cell implantation (designated as Day 0 of the study), mice were randomized into four groups of 8 animals each and treated with vehicle, Fulvestrant (250 mg/kg, subcutaneous injection, once a week), or SCR-6852 (3, or 10 mg/kg, oral gavage, daily). Survival of mice was evaluated until Day 60. Mice were euthanized with weight loss exceeding 20% or moribund. On Day 60, all the mice remaining alive were euthanized. Before euthanasia, the mice were perfused with 4% paraformaldehyde and the brain tissues were collected for H&E staining using AUTOSTAINER XL (Leica, Wetzlar, Germany).

Assessment of uterotrophic activity

Female SD rats at 3 weeks of age with bodyweights ranging from 62.3 to 82.3 g were randomized into three groups of 8 animals each and treated with vehicle, tamoxifen (60 mg/kg), or SCR-6852 (10 mg/kg) by oral gavage once daily for three consecutive days. Twenty-four hours after the final dose, all animals were euthanized. Body weights and wet uterine weights were recorded for each animal. Fresh uterine tissue from each rat was fixed in 4% paraformaldehyde, dehydrated by HistoCore PEARL (Leica), and embedded by HistoCore Arcadia H+HistoCore Arcadia C (Leica). Sections were cut at 4 μ m and stained with 0.1% toluidine blue O. The thickness of endometrial epithelium was measured using Leica Aperio CS2 with ImageScope \times 64 program (Leica). The mean of five measurements per specimen was calculated.

Brain distribution studies

MCF-7 tumor bearing mice were orally administered with multiple doses of SCR-6852, AZD-9833 or GDC-9545 once a day at 10 mg/kg, respectively, or subcutaneously administered with fulvestrant at 250 mg/kg once per week. The blood and brain tissues were collected at 24 h post the last dose. In addition, three male Sprague–Dawley (SD) rats (200–300 g, 6–8 weeks old, Beijing Vital River) were orally administered with 10 mg/kg SCR-6852 and the blood and brain tissues were collected at 24 h post-dose. In a 14-day repeated oral dose-range finding study of SCR-6852 conducted in beagle dogs at 10 mg/kg/day, the blood and brain tissues were collected at 24 h post the last dose to determine the brain penetration of SCR-6852 in dogs. All blood was collected in K2-EDTA tubes and plasma was obtained by centrifuging the blood at 3200 rpm for 10 min at 4 $^{\circ}$ C and the brain was rinsed with water and blotted to remove superficial meninges. Plasma and brain samples were stored at -80° C until LC–MS/MS analysis which was performed on an Acquity UPLC system (Waters, USA) coupled to an AB SCIEX Triple Quad 6500+ System.

Statistical analysis

Statistical and graphical presentations were performed using IDBS XLfit and GraphPad Prism 9. For cell proliferation assays, the IC₅₀ was calculated by fitting a dose–response curve using a nonlinear regression model with a log(inhibitor) vs response curve fit. Relative IC₅₀, determined as the concentration where 50% of the maximal response is observed, was calculated by the IDBS XLfit curve fitting software. Tumor growth inhibition (TGI) at the end of the study was calculated using the following formula: $TGI (\%) = (1 - (V_t(\text{treatment group}) - V_0(\text{treatment group})) / (V_t(\text{vehicle group}) - V_0(\text{vehicle group}))) \times 100\%$; V_0 is the

tumor volume of the animal when treatment starts; V_t is the tumor volume of the animal someday after treatment. The tumor volumes were analyzed by two-way ANOVA followed by Tukey’s multiple comparisons tests. The survival curves were analyzed by Log-rank (Mantel-Cox) test. The uterine relative weights and the thickness of endometrial epithelium were analyzed by one-way ANOVA followed by uncorrected Fisher’s LSD. P -values < 0.05 were considered statistically significant.

Results

SCR-6852 demonstrates a fully antagonistic binding model to ER α

Based on the molecular binding mode of ER α with its ligand, a series of SERD molecules were rationally designed through the structure-based optimization strategy, such as SCR-6139, SCR-6515, and SCR-6852. According to the co-crystal structure of ER α and its ligand ((R)-2,3-dimethyl-2,3,4, 9-tetrahydro-1 h-pyrido [3,4-b] indole), this particular ligand demonstrated two key hydrogen bonds with Glu353 and Asp351,

which were critical for antagonistic binding. Besides, additional hydrophobic interactions and Pi-Pi interactions among residues Phe40 and CH-Pi interactions with Thr347, Leu525 and Ile424 were also very important (Fig. 1a). Comparison with the well-defined binding mode of ER α - ligand, we identified that Fulvestrant, SCR6515, and SCR6139 were not only able to maintain the primary hydrogen bonding interactions with Glu353 residue but also increase the hydrogen bonding interactions with Asp351 and Val533 (Fig. 1, Additional file 1: Fig. S1). The docking scores are comparable at -9.59, -11.17, and -9.72 kcal/mol for Fulvestrant, SCR6515, and SCR6139, respectively (Table 1). This molecular docking indicated that both SCR-6515 and SCR-6139 are likely to have similar antagonistic effects to Fulvestrant. Additionally, SCR-6852, an analogue of SCR-6515 and SCR-6139 exhibited a similar binding model and equal level docking score of SCR6515 and SCR6139. The docking score for SCR-6852 is -10.38 kcal/mol (Table 1). Further, SCR-6852 also maintained the key interactions appeared in the

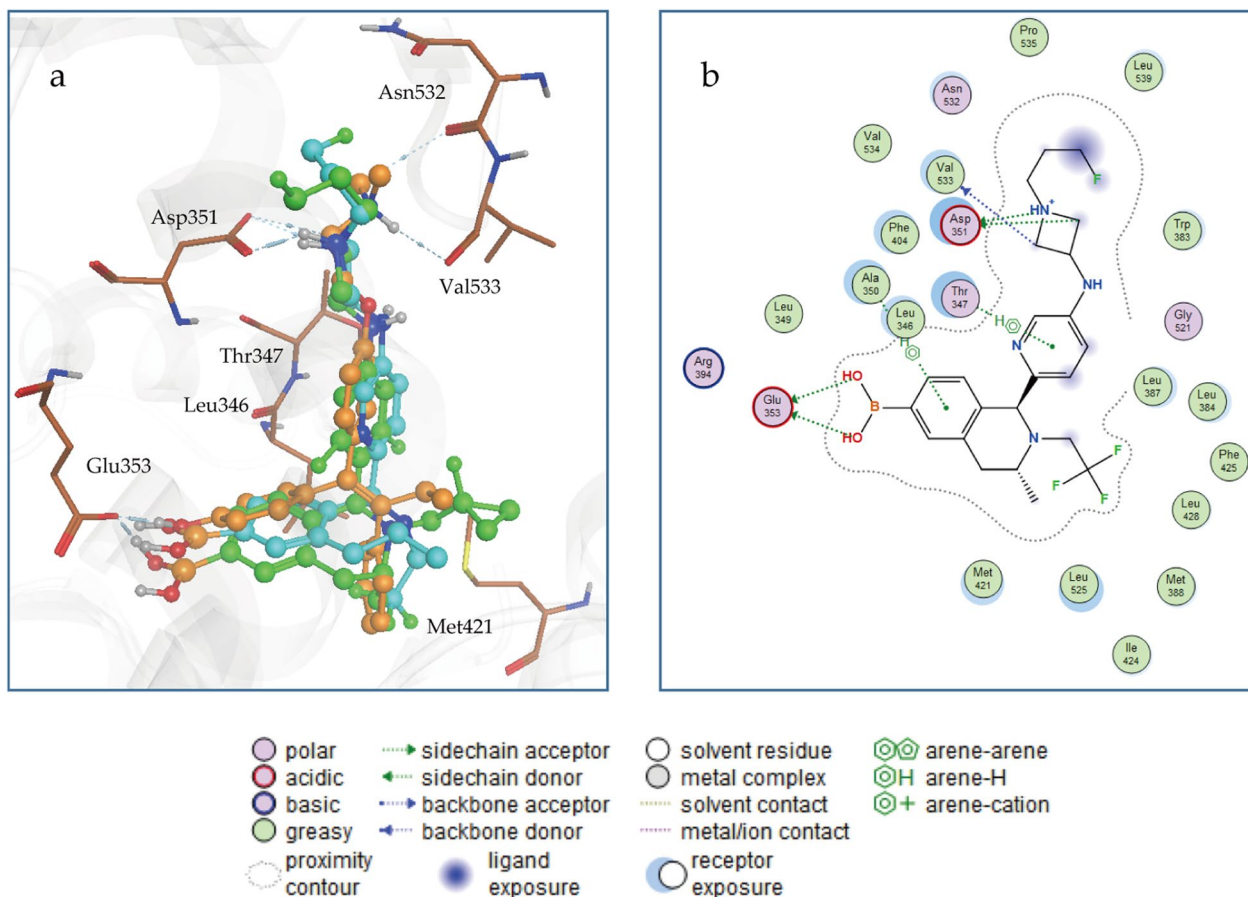


Fig. 1 Docking diagram of SCR6139, SCR6515, and ER α -LBD complex. **a** SCR6139 and SCR6515 were docked to ER α -LBD complex (PDB: 6Z0Q; the crystal ligand in 6Z0Q (carmine), SCR6139 (blue), SCR6515 (green)). **b** Schematic diagram of two-dimensional interaction for SCR6139

Table 1 The docking score for the six ER α antagonists

	6ZOQ-lig	4-hydroxy tamoxifen	SCR6139	SCR6515	Fulvestrant	SCR6852
DS*(kcal/mol)	- 8.85	- 6.83	- 9.72	- 11.17	- 9.59	- 10.38

*: Docking score used in MOE (GBVI/WSA dG)

Co-crystal, such as the hydrogen bonds with Asp351 and Val533 and Pi-Pi interaction with residue Phe404. These results suggested SCR-6852 probably could be a pure ER α antagonist. Furthermore, the antagonistic activities were identified on a nuclear translocation assay, SCR-6852 exhibited the pure antagonism activity with the maximal inhibition of 100% comparable to Fulvestrant (Additional file 1: Fig. S2). Meanwhile, the high selectivity (about 500-fold) of SCR-6852 against Progesterone Receptor (PR) or Androgen Receptor (AR) was obtained, and no obvious agonist/antagonist activities on several safety-relevant off-targets (Additional file 2: Table S1, SAFERYscan E/IC50 ELECT-78 assays, by Eurofins Discovery).

SCR-6852 effectively degrades ER α and inhibits the growth of ER+ cell lines

Cellular data demonstrated that all these compounds, SCR-6139, SCR-6515 and SCR-6852 effectively induce ER α degradation in MCF7 breast cancer cells (ER α wild-type, wt), as shown in (Fig. 2a, Table 2, Additional file 1: Fig.S3). In particularly, SCR-6852 induced ER α degradation at the nanomolar concentrations (half maximal degradation concentration [DC₅₀] of 1.05 ± 0.35 nmol/L), with the maximal ER degradation activity (Dmax) of 57.6%. In comparison of Fulvestrant, SCR-6852 demonstrated comparable ER α degradation capacity either at the DC₅₀ or at the Dmax of degradation. The maximal ER α degradation activities of SCR-6852 were further evaluated in a panel of ER+ breast cancer cell lines. As shown in Fig. 2b, SCR-6852 achieved a consistent maximal ER α degradation rate across those lines and showed comparable activities to Fulvestrant. In parallel, AZD9496, an incomplete ER α degrader showed a less potency ER α degradation rate. Consistent with ER α degradation, SCR-6852 strongly inhibited those ER+ lines proliferation and achieved comparable activities with Fulvestrant either at IC₅₀ or at the Emax (Fig. 2c). Although AZD9496 showed comparable activities at IC₅₀, it achieved lower maximal anti-proliferation rate in two cell lines, CAMA-1 and HCC1500. In addition, 4-OH Tamoxifen (4-OHT), a Selective ER Modulator (SERM) showed less potent than all tested SERDs, suggesting ER α degrader rather than antagonist would achieve superior efficacy. Furthermore, SCR-6852 exhibited no inhibitory effect on the growth of ER- cell line (SK-BR-3) even at a high concentration

(2 μ M/L), suggesting the high selectivity of SCR-6852 for ER α -dependent tumor cells (Additional file 1: Fig. S4).

ER α mutations with gain-of-function capabilities have been shown to be one of the resistance mechanisms to anti-ER α therapies in patients with breast cancer [4]. SCR-6852 strongly inhibited the proliferation of ER α wt (MCF7 parental) and ESR1 mutants Y537S/ D538G (MCF7 ESR1 Y537S or MCF7 ESR1 D538G) cell lines, which was comparable with Fulvestrant (Fig. 2d). Meanwhile, comparison with RAD1901, an approved oral SERD recently, SCR-6852 was more potent on inhibition of cell growth both in ESR1 WT and mutant lines (Fig. 2d). Furthermore, the degradation activities of SCR-6852 on ER α in ESR1 Y537S mutant and the effects of the downstream signals were determined by western blot. SCR-6852 dose-dependently degraded both WT (Fig. 2e) and Y537S mutant (Fig. 2f) ER α in cells, which showed comparable potency with Fulvestrant. The key regulators of ER signal axis, cyclin D and phosphorylated retinoblastoma (pRb) were both downregulated following the ER α degradation (Fig. 2e, f and Additional file 3).

The estrogen receptor is a ligand-inducible transcription factor that regulates the transcription of numerous genes. To explore the impact of SCR-6852 on the ER α -target genes transcription, transcriptomic analysis was performed in MCF7 cells in the presence of E2, SCR-6852, Fulvestrant, and 4-OHT, respectively. MCF7 were hormone-deprived before ER ligand treatment and then differentiated gene transcription was compared to that of E2-stimulation. Results from Principal component analysis (PCA) showed that the gene transcriptomic data in cells treated with SCR-6852 and Fulvestrant, respectively, were clustered and differed from the 4-OHT treatment group. It was observed that 4-OHT partially promoted transcription of some ER target genes. Results from transcriptomics showed that 5.8% of the genes induced by E2 also being upregulated by 4-OHT (foldchange > twofold), and 59.1% of E2-induced genes were suppressed by 4-OHT (Fig. 3a, b, Additional file 2: Table S2). In contrast, SCR-6852 and Fulvestrant inhibited the transcription of 78.5% and 76.4% of E2-induced genes, respectively. Furthermore, two typical ER target genes, *AGR3* and *GREB1* were chosen to test the effect of SCR-6852 on the E2-induced gene transcription by RT-QPCR in more ER+ cell lines. Consistent with transcriptomic data from MCF7, both Fulvestrant and SCR-6852

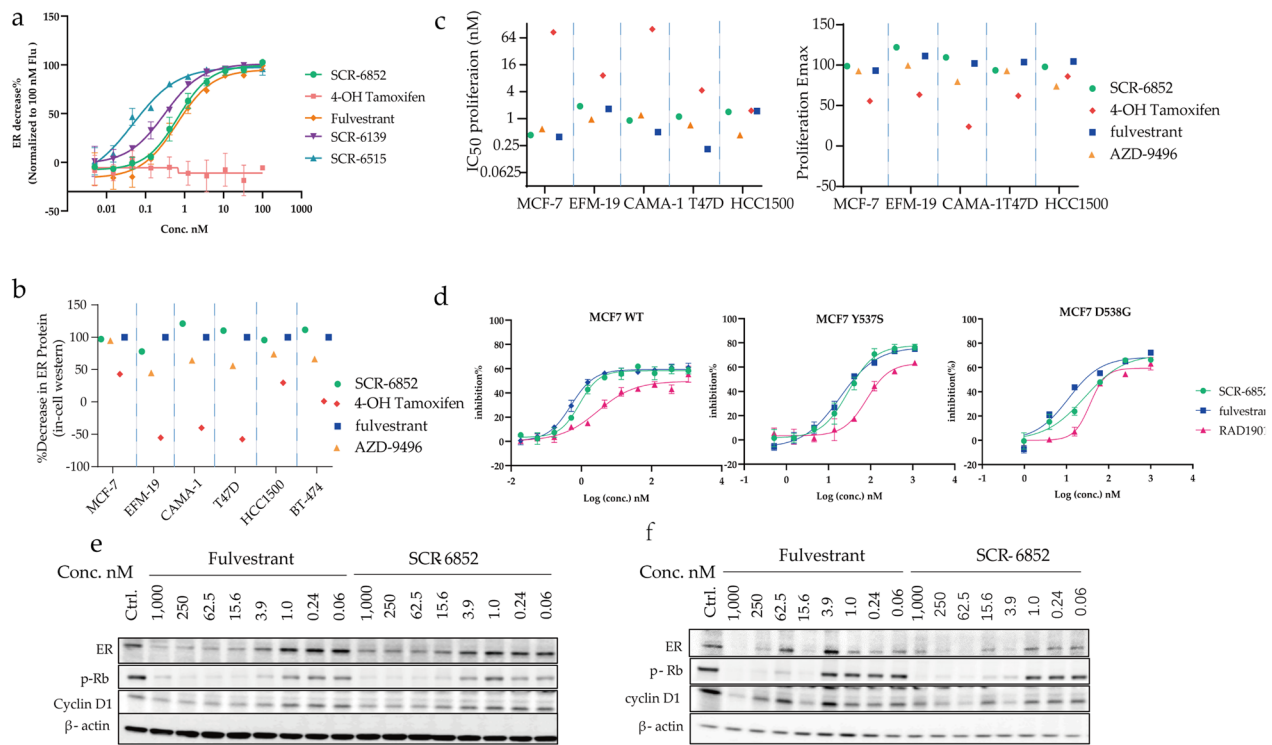


Fig. 2 SCR-6852 is a potent SERD to induce ER α degradation and anti-proliferation of ER+ breast cancer cell lines. **a** The comparison of in-house compounds potency to fulvestrant or 4-OH-tamoxifen by In-Cell Western Assay (ICW). MCF7 cells were seeded in a 384-well plate and linear-dilution compounds were administrated in duplicate for each treatment. After incubation for 24 h, Cells in the assay pate were treated as described in methods. ER α levels were quantified by immunofluorescence assay. 100% normalized to fulvestrant activity at 100 nM. Data are given as mean \pm SEM. **b** The maximal ER α degradation across an ER-positive cell panel was evaluated in an In-cell Western assay. Cells were dispended into 96-well plates and incubated for 24 h with compounds (100 nM) treatment. Cellular ER α levels in each treated well were quantified by immunofluorescence assay. 100% normalized to fulvestrant activity at 100 nM. **c** The comparison of cell viability between SCR-6852, AZD-9496, fulvestrant, or 4-OH-tamoxifen activity, across an ER-positive cell panel. Cells were seeded in 384-well plates and treated with linear-dilution compounds for 7 days of incubation. Cell viability was assessed using CellTiter-Glo. Cell growth inhibition is presented as a percentage of CellTiterGlo activity relative to the vehicle control. 100% normalized to maximal fulvestrant activity. **d** The comparison of cell viability between SCR-6852, fulvestrant or RAD-1901 activity, respectively, in MCF7 cells with ER WT, or mutant ESR1 Y537S, or mutant ESR1 D538G with the same operation as above. **e-f**, The evaluating of ER α level, as well as RB phosphorylation and cyclin D1 as ER targets by western blot, in MCF7 ER. WT (**e**) and ER. Y537S cells (**f**). Cells were seeded in 6-well plates and treated with linear-titration Fulvestrant or SCR-6852 for 5 days of incubation. Then cells in each well were collected and the targeting proteins in lysate supernatant were detected by WB

Table 2 In vitro properties of SCR-6852

	ER α degradation assay			Viability assay		
	DC ₅₀ nM	D _{max} [% Ful.]	D _{max} [% Veh.]	IC ₅₀ nM	E _{max} [% Ful.]	E _{max} [% Veh.]
MCF-7 WT						
Fulvestrant	0.93	97.69	56.04	0.40	97.88	49.60
SCR-6852	1.05	100.45	57.61	0.72	96.22	48.96
SCR-6515	0.08	97.83	66.81	0.29	103.00	64.15
SCR-6139	0.31	101.13	69.02	0.40	98.77	58.83
MCF-7 Y537S						
Fulvestrant	32.05	87.09	26.38	16.29	95.49	65.05
SCR-6852	47.32	99.57	30.17	27.6	100.96	68.78
MCF-8 D538G						
Fulvestrant				11.10	106.1	68.57
SCR-6852				26.96	109.5	70.8

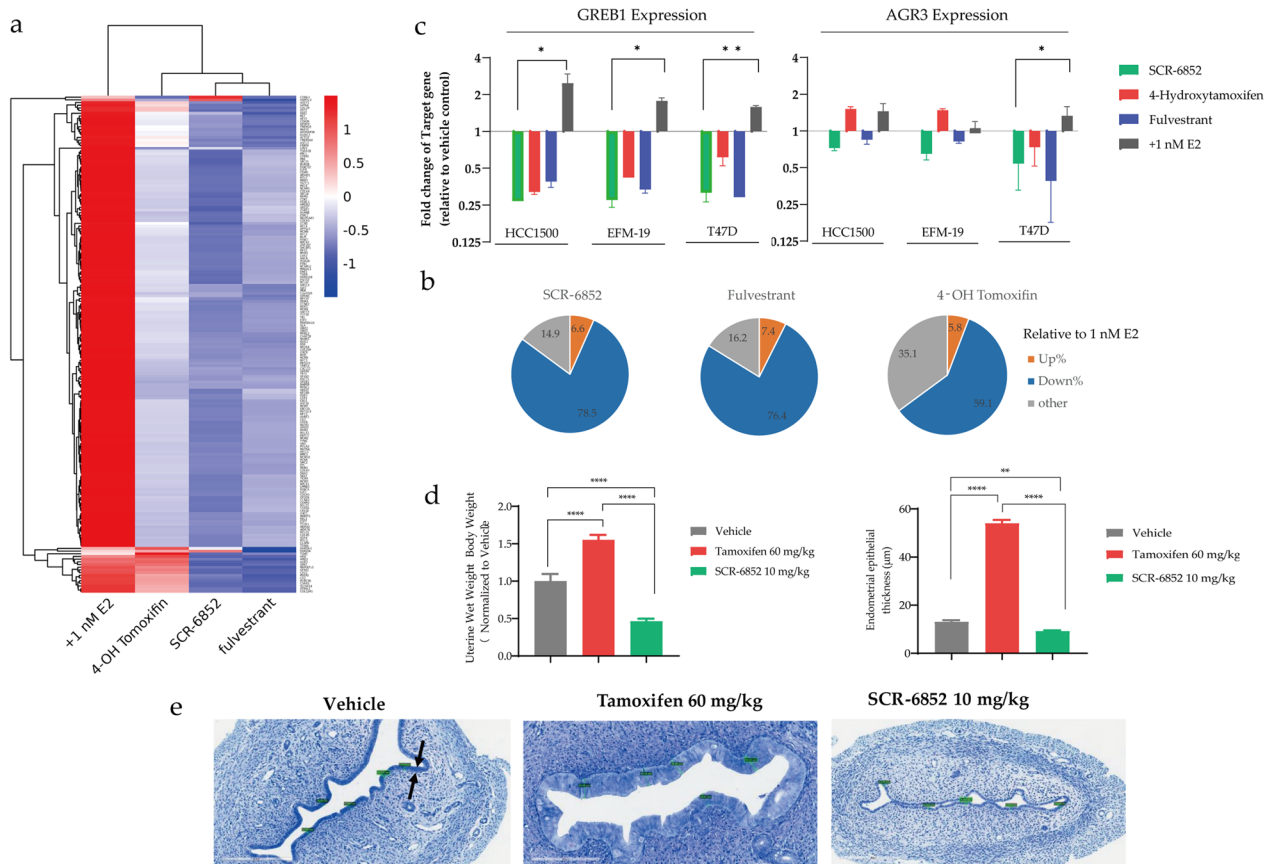


Fig. 3 Effects on ER target genes expression and uterine tissue of SCR-6852. **a** Differential expression analysis from RNA-seq. MCF7 with hormone-deprived pre-treatment were administrated ER ligands or not present with 1 nM E2 stimulation for 24 h incubation in a 12-well plate. Total mRNA was isolated from treated cells and sequenced on an Illumina HiSeq X Ten platform. FPKM of each gene was calculated using Cufflinks and Differential expression genes analysis by using the DESeq (2012) R package. Four separate clusters were obtained. Rows show genes up- or downregulated by E2 relative to control (> twofold, FDR < 0.05), or by each ER ligand. **b** Summary of the transcriptional consequences. In orange is the percentage of upregulated genes compared with E2 in total test genes by experimental ligand (> twofold, FDR < 0.05), and those in blue are downregulated. **c** ER-target gene *GREB1* or *AGR3* expression analysis. T47D EFM-19 and HCC1500 cells were grown in RPMI media supplemented with 10% charcoal-stripped FBS for 14 days and then treated with ER antagonist (1 μ M) or DMSO in the presence E2 (1nM) stimulation for 24 h before RNA isolation and gene expression analysis as described in methods. Asterisks show one-tail *t*-test *p*-values. *P*-values: * *P* < 0.05; ** *P* < 0.01. **d-f** Effect of SCR-6852 on uterine tissue. 21 days old SD rats were dosed with a vehicle, 60 mg/kg tamoxifen or 10 mg/kg SCR-6852 orally every day for three days. The uteruses were harvested 24 h after the final doses and stained by toluidine blue. Endometrial height was assessed from the basement membrane to the luminal border (scale bar in green lines: 200 μ m), Arrows indicate the uterine epithelium (**e**). Wet uterine weight normalized to body weight and Endometrial thickness were digitally measured and plotted in the graph in figure (**d** and **e**). * *P* < 0.05; ** *P* < 0.01; *** *P* < 0.001; **** *P* < 0.0001

significantly downregulated both *AGR3* and *GREB1* transcription in T47D, EFM-19, and HCC1500 cells (Fig. 3c). while a significant increase of *AGR3* transcription was observed in both EFM-19 and HCC1500 by 4-OH-tamoxifen treatment. Taken together, SCR-6852 is a pure ER α antagonist.

Since the activity of ER ligands could be tissue-dependent, we next evaluated the effects of SCR-6852 on the uterus of juveniles in rats. As shown in Fig. 3d, Tamoxifen at 60 mg/kg resulted in a significant

increase in relative uterine wet weight (*P* < 0.0001). In contrast, oral administration of SCR-6852 at 10 mg/kg decreased the uterine wet weight instead (*P* < 0.0001). Treatment-dependent changes in the uterine tissue were further investigated by quantitative microscopic histological analysis. As shown in Fig. 3e and f, SCR-6852 at 10 mg/kg decreased the endometrial epithelial thickness compared to vehicle treatment (*P* < 0.01), while tamoxifen at 60 mg/kg significantly increased the endometrial epithelial thickness (*P* < 0.0001). These data suggested that SCR-6852 completely antagonized the ER signal axis in the uterine tissue.

SCR-6852 exhibits superior anti-tumor activities in the ER+ subcutaneous xenograft breast cancer tumors

The in vivo antitumor activities of SCR-6852 were evaluated in two ER+breast cancer subcutaneous tumor models. SCR-6852 dose-dependently inhibited MCF7 tumor growth (Fig. 4a), with TGIs being 45.22%, 116.33%, 123.26%, and 123.80% at 0.3, 1, 3, and 10 mg/kg, respectively ($P < 0.0001$ for all SCR-6852 treatment groups compared to vehicle group). Meanwhile, SCR-6852 at the dosages of 1, 3, and 10 mg/kg all showed superior anti-tumor activities than Fulvestrant at 250 mg/kg (TGI of 28.84%, $P < 0.0001$), and one out eight mice with

tumor-free were observed in 1 mg/kg and 3 mg/kg SCR-6852 treatment groups, respectively (Fig. 4b). Treatment of SCR-6852 was well tolerated with no significant body-weight loss in animals (Additional file 1: Fig. S5a). Furthermore, to fully understand the effects of SCR-6852 on ER signal axis in tumors, a separate experiment was carried out for PD marker detection. The ER-target gene *PGR* [31] was significantly reduced in SCR-6852 treatment groups (> 1.8 mg/kg groups, $P < 0.001$) (Additional file 1: Fig. S6).

Additionally, in another ER+breast cancer cell T47D subcutaneous xenograft tumor model, SCR-6852

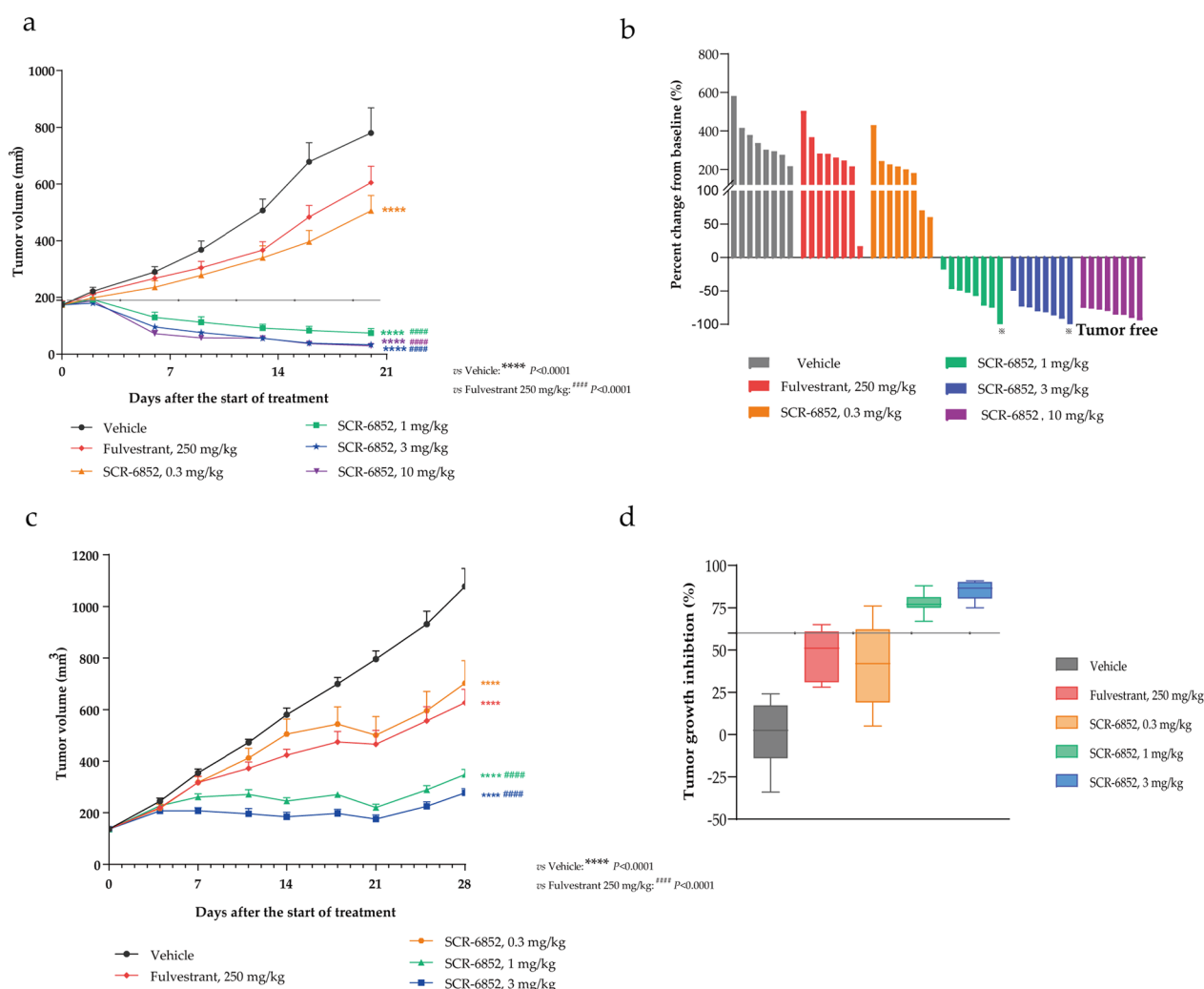


Fig. 4 Antitumor activity of SCR-6852 in xenograft models. **a–b** ER-positive cancer cell line MCF-7 was implanted in Balb/c nude mice with 17β-Estradiol to stimulate tumor growth. Animals were treated with SCR-6852 (0.3, 1, 3, or 10 mg/kg, respectively, daily, orally) or 250 mg/kg fulvestrant (subcutaneous injection once a week). Tumor volume was evaluated twice per week until the study endpoint. **a** Mean tumor volume ± SEM. **b** Percent change in tumor volumes from individual animals from the start of treatment to the end of treatment. **c–d** T47D subcutaneous xenograft model was also used. Tumor-bearing Balb/c nude mice received the vehicle, 250 mg/kg fulvestrant, or SCR-6852 0.3, 1, 3 mg/kg (QD) (n=8/group). **d** Tumor growth inhibition for each treatment group relative to vehicle at end of treatment. The error bars represent the standard error of the mean (SEM). **** $P < 0.0001$ versus vehicle, #### $P < 0.0001$ versus Fulvestrant

demonstrated robust tumor growth inhibition with TGI of 77.47%, and 85.04% at 1 and 3 mg/kg, respectively, presenting superior anti-tumor activities than fulvestrant at 250 mg/kg (TGI of 48.35%, $P < 0.0001$, Fig. 4c and d). Even at a very low dose, 0.3 mg/kg, SCR-6852 demonstrated comparable efficacy with Fulvestrant at 250 mg/kg (TGI: 39.87% Vs 48.35%). Again, SCR-6852 was tolerated well, and there was no significant body weight loss observed in all test animals (Additional file 1: Fig. S5b).

SCR-6852 has high brain penetrability and effectively suppresses ER+ tumor growth in an intracranial tumor model.

The inhibitory activity of SCR-6852 on the tumor metastasis in the brain was evaluated in an intracranially orthotopic xenograft model. The ER+MCF7 cells were intracranially implanted and anti-tumor efficacy was evaluated using survival as the primary endpoint based on the Kaplan–Meier survival analysis. As shown

in Fig. 5a and Additional file 1: Fig.S5c, SCR-6852 dose-dependently increased the mice survival, and the median survival time of mice received 10 mg/kg of SCR-6852 treatment significantly increased (not reached) compared to the vehicle group (26.5 days) ($P < 0.001$). Notably, all mice that received 10 mg/kg of SCR-6852 treatment survived by the end of the study (Day 60). In parallel, mice received 250 mg/kg of Fulvestrant treatment had no significant difference in median survival time compared to vehicle (27 vs. 26.5 days, $P > 0.05$), although it achieved moderate anti-tumor activity in subcutaneous tumors. Next, infiltration and proliferation of tumor cells in these mice’s brain tissues were evaluated by H&E staining. The brain tissues were harvested when mice are sacrificed due to tumor progression or at the end of the study if the mice remained healthy (Day 60). As shown in Fig. 5b, significant tumor cells infiltration and destruction of physiological structure were observed in vehicle, Fulvestrant, and 3 mg/kg of SCR-6852 treatment groups, while only a

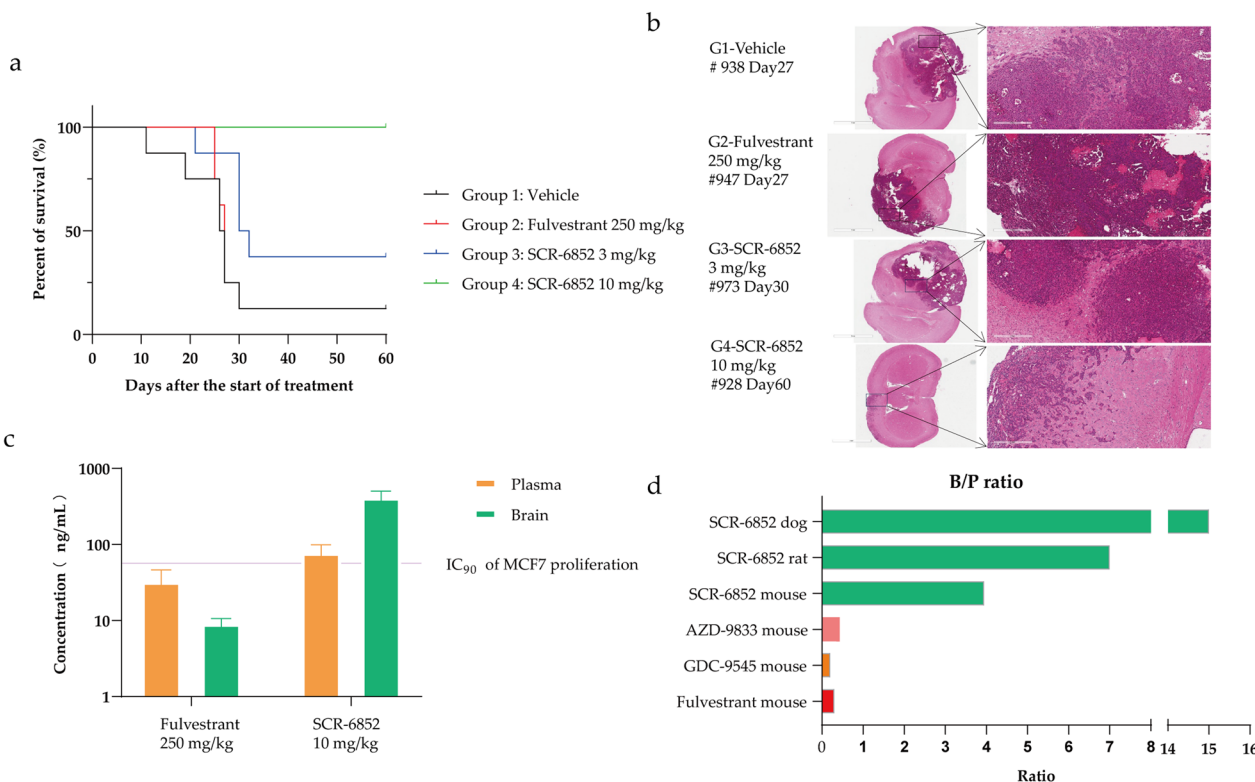


Fig. 5 BBB permeability and in vivo activity. **a–b** Female NPG mice were implanted with MCF-7 cells intracranially. Eight days after tumor cell implantation (designated as Day 0 of the study), mice were treated with vehicle, 250 mg/kg fulvestrant (administration as described above), 3 or 10 mg/kg SCR-6852 (QD, $n = 8$ /group), and survival of the animals were recorded. The survival curves of the animals are shown (**a**). Representative images of the brain tissue H&E staining are also shown (**b**). The day that the brain tissues were collected for the representative images is indicated in the graph. Scale bar: 3 mm or 300 μ m. **c** The intracranial MCF7 (orthotopic) xenograft mice were treated with SCR-6852 or Fulvestrant for 8 days, and the tissues were collected 24 h after the last dose. SCR-6852 or Fulvestrant concentration in the brain or plasma was determined by LC–MS. Brain conc./plasma conc. was presented as a B/P ratio. **d** The CD1 IGS mice/rat / Beagle were administrated with multiple doses of SCR-6852 or other compounds, and the tissues were collected at 24 h after the last dose as described in methods. relative compound concentration in the brain or plasma was determined by LC–MS. Brain conc./plasma conc. was presented as a B/P ratio

very small amount of tumor cell infiltration was observed in the brain tissues from 10 mg/kg of SCR-6852 group, confirming the robust anti-tumor efficacy of SCR-6852 in mice's brain tissues.

Next, the exposure of SCR-6852 and Fulvestrant in brains were determined in the above intracranial MCF7 (orthotopic) xenograft model in an independent assay. Mice were administrated with SCR-6852 (10 mg/kg, oral gavage, daily, from Day 0 to Day 7) or Fulvestrant (250 mg/kg, subcutaneous injection, once a week, on Day 0 and Day 7) (Fig. 5c), respectively, then the plasma and brain tissues were collected at 24-h post-last dose. The drug concentrations were determined by LC-MS/MS. The concentration of SCR-6852 in plasma was 78 ± 21 ng/ml, and in brain was 419 ± 82 ng/ml. SCR-6852 exhibited high brain exposure with a B/P (brain/plasma) ratio of more than 5 folds, while Fulvestrant tended to be distributed in plasma with a low B/P ratio of fewer than 0.5 folds. In addition, SCR-6852 concentration in brain was much higher than the IC_{90} value of anti-proliferation determined in MCF7 cells (56.68 ng/mL, corrected by 98.8% PPB), suggesting the robust anti-tumor activity in intracranial tumors correlates well to the exposure of drug in brains.

In addition to mice, the brain exposure of SCR-6852 in rats and dogs was further determined. Animals received an oral administration of SCR-6852 at 10 mg/kg, then plasma and brain tissues were collected at 24-hour after 14 days of dosing. As shown in Fig. 5d, SCR-6852 demonstrated extremely high exposure in both species with a B/P ratio of 7 folds in rats and 15 folds in dogs, respectively. In parallel, the brain exposure of some ER degraders, including Fulvestrant and oral SERDs, AZD-9833, and GDC-9545 were compared with SCR-6852 in mice side by side. Results showed that neither Fulvestrant nor those oral SERDs could effectively distribute to brains with the B/P ratio less than onefold. Taken together, SCR-6852 demonstrated high brain exposure in three preclinical species, including rodents and non-rodents.

SCR-6852 synergistically inhibits ER + tumor growth in combination with a CDK4/6 inhibitor in vitro and in vivo
Combination of the CDK4/6 inhibitor (CDK4/6i) and endocrine therapy (ET) has become standard treatments following the progression of initial AI monotherapy. Here we observed the synergistically anti-tumor effects of SCR-6852 in combination with a CDK4/6 inhibitor, Palbociclib. The synergy analysis displayed that the synergism in preventing the cells proliferation as SCR-6852 combined with Palbociclib was demonstrated with an average synergy score of 11 (Fig. 6a). And the combination with SCR-6852 significantly improved the anti-proliferation activity of Palbociclib with the apparent tenfold

shift of IC_{50} . Further cell cycle analysis showed that the combination of SCR-6852 and Palbociclib significantly increased the cell numbers in the G1 phase compared to SCR-6852 or Palbociclib alone. And accompanying the decrease of cell numbers in the S or G2/M phase was also observed (Fig. 6b).

The combination of SCR-6852 and Palbociclib was further assessed in the MCF-7 subcutaneous tumors. As shown in Fig. 6C, the combination of SCR-6852 (0.3 mg/kg) and Palbociclib (40 mg/kg) significantly enhanced the tumor growth inhibition compared to monotherapy ($P < 0.0001$, TGI: 100.10% vs. 53.35% vs. 66.34%; Groups: combo vs. SCR-6852 vs. Palbociclib). Similarly, the combination of 1 mg/kg SCR-6852 and 40 mg/kg Palbociclib also showed improvement in tumor growth inhibition compared to monotherapy ($P < 0.05$, TGI: 113.76% vs. 92.70% vs. 66.34%; combo vs. SCR-6852 vs. Palbociclib). Also, all treatments were well tolerated (Additional file 1: Fig. S5d).

Discussion

The ER-target therapy that directly opposes the mitogenic action of estrogen or that block estrogen synthesis is an approved strategy for the treatment of ER-positive breast cancer. Here we identified a series of novel ER degraders such as SCR-6139 and SCR-6852. The modeling study of these compounds binding to ER α revealed that the molecular interactions of our compounds with the ER α ligand binding domain were nearly identical to those of Fulvestrant, indicating that these compounds were ER α degrader with potential pure-ER antagonistic activity. The following cell-based efficacy studies well demonstrated that one of those, SCR-6852, was a potent SERD that induced ER degradation and inhibited ER+ cancer cell growth with a high potency comparable with Fulvestrant. Furthermore, in a parallel comparison assay, SCR-6852 displayed greater capabilities in ER α degradation and anti-proliferation than 4-OHT and AZD-9496 in multiple ER+ breast cancer cell lines, indicating SCR-6852 was different from 4-OHT or AZD-9496 and similar with Fulvestrant. And the following transcriptional signatures also revealed that SCR-6852 cluster close to Fulvestrant, while tamoxifen regulated a subset of genes in a similar manner to estradiol. Particularly, the agonist activity on *AGR3* expression of tamoxifen was observed, and on the contrary, SCR-6852 downregulated this gene expression to the maximum level. Tamoxifen, as a SERM, had been well demonstrated robust antagonist activity in the breast epithelium but mimicked the agonist effect of estrogen in bone, endometrium, and serum lipid profiles [32–34]. Our study also verified that tamoxifen acted as a pro-estrogen agonist by causing the endometrium to appear thickened in immature rats, however, SCR-6852

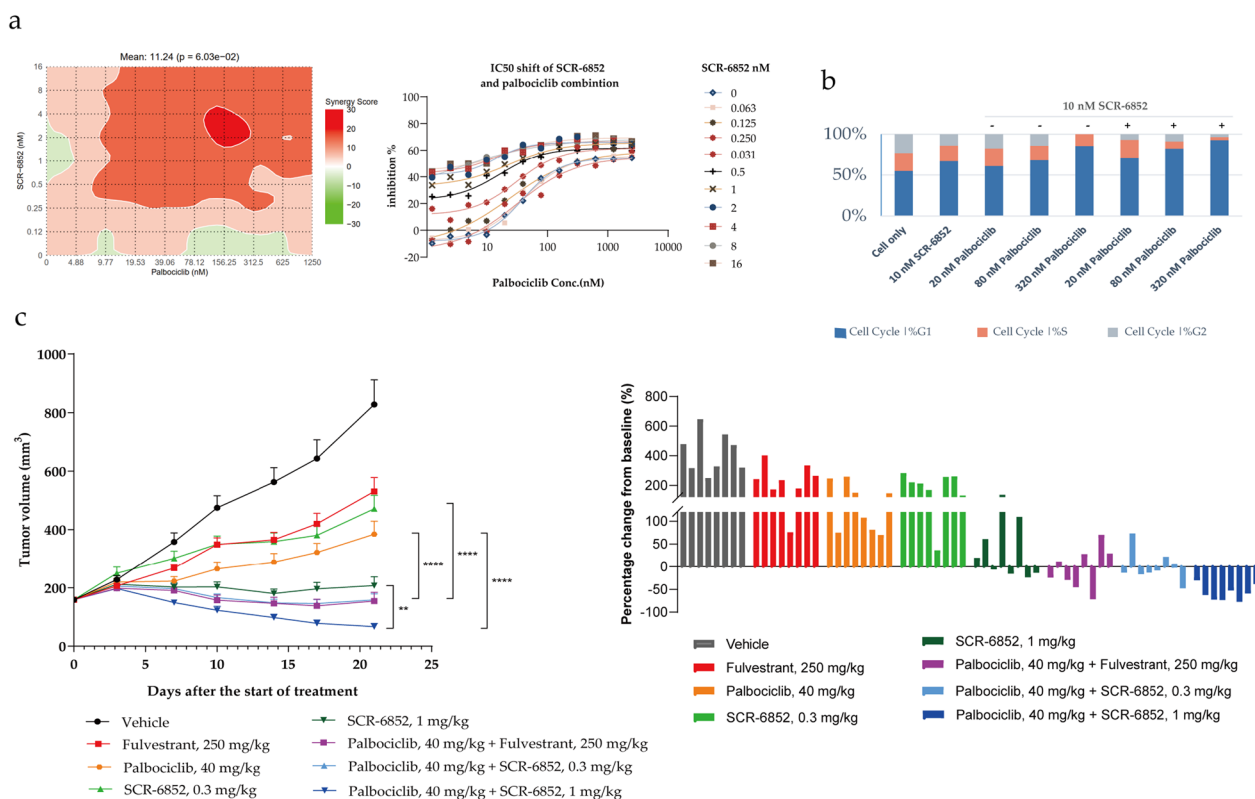


Fig. 6 The synergistic effects for SCR-6852 combined with CDK4/CDK6 inhibitor in vitro and in vivo **a** MCF7 were treated with increasing concentrations of SCR-6852 and/or Palbociclib for 7 days in a 384-well plate. Cell viability was measured using Cell TiterGlo assay. Combination analysis with Loewe’s additivity mode by SynergyFinder (<https://synergyfinder.fimm.fi>) displayed surfaces of synergy on the left; red indicates synergy (synergy score > 0) and green indicates antagonism (synergy score < 0). The potency shift of Palbociclib combined with a serial SCR-6852 dosing were represented graphically as dose–response curves, on the right. **b** MCF-7 cells were treated with SCR-6852 or combined Palbociclib for 40 h, and cell cycle distribution was analyzed by Flow cytometry. The result of one representative assay from three similar independent experiments is shown. The percentages of cells in G1, S, and G2/M were shown as indicated. **c** The MCF-7 tumor-bearing Balb/c nude mice received the vehicle, 250 mg/kg Fulvestrant, 40 mg/kg Palbociclib, 0.3 mg/kg SCR-6852, 1 mg/kg SCR-6852, or combination treatments as indicated in the graph (n = 8/group). The error bars represent the standard error of the mean (SEM). ****P < 0.0001; **P < 0.01 combination versus single as indicated

decreased the uterine wet weight and endometrium thickness instead. This antiestrogenic effect of SCR-6852 was observed in Fulvestrant treatment in a previous report [35]. The above data demonstrated our compound SCR-6852 is a pure ER antagonist.

The acquisition of ligand-independent *ESR1* mutations during aromatase inhibitor therapy in metastatic ER+ breast cancer was a common mechanism of hormonal therapy resistance [36]. The most common mutations in *ESR1* occurred at the Y537 and D538 residues, and the Y537S mutation was relatively more resistant to growth inhibition when treated with ER antagonists compared with D538G and WT [37]. In the MCF7 cells with *ESR1* Y537S mutation, SCR-6852 efficiently induced the mutant ERα degradation and demonstrated comparable anti-proliferation activities with Fulvestrant. Meanwhile, compared with RAD1901, SCR-6852 displayed more activity of anti-proliferation of both *ESR1*

WT and Y537S/D538G mutant stain. Elacestrant was currently approved, and the efficacy and safety were evaluated in EMERALD (NCT03778931). In this study patients including WT or mutant *ESR1*, progressed on up to 2 lines of ET with a CDK4/6 inhibitor, and were randomized to either Elacestrant or standard-of-care ET (Fulvestrant, Anastrozole, Letrozole, or Exemestane). The positive clinical results were disclosed in ASCO, 2022. EMERALD met both of its pre-specified primary endpoints of progression-free survival (PFS) in the overall population and in patients with the *ESR1* mutation (*mESR1*) compared to SOC endocrine monotherapy. The PFS rate at 12 months with Elacestrant was 22.32% vs. 9.42% with SOC in the overall population and 26.76% vs. 8.19% in the *ESR1* mutation population. These clinical trial data showed that Elacestrant reduced the risk of disease progression or death by 30% in all patients and by 45% in patients with *ESR1* mutation. This significant

efficacy in the Elacestrant arm demonstrated that an oral SERD was useful and better than a Fulvestrant for patients with *ESR1* mutants.

The treatment of breast cancer brain metastases is especially challenging. The blood–brain barrier restricts the diffusion of many drugs into the brain inclusive of limiting highly permeable drugs by active efflux transporters expressed in BBB. Therefore, effective exposure to drugs in the brain is critical to treat brain metastasis. Abemaciclib [38] significantly increased survival in a rat orthotopic U87MG xenograft model by confirming a sufficient unbound brain concentration with a target engagement ratio (the ratio of the unbound brain concentration to the in vitro enzyme IC_{50}) of 3.3–14.3 for approximately 12 h in mice dosed with 30 mg/kg. And Buparlisib ([39]) is demonstrated as a brain penetrable panPI3K inhibitor for high brain accumulation (B/P ratio > 1.5) and efficient intracranial target inhibition at clinically achievable. These two clinical agents are now being investigated in clinical trials for BCBM treatment ((NCT02675231, NCT02437318) [40]. In this study, we revealed that SCR-6852 highly accumulated in the brain in mice. The brain concentration was more than seven-fold IC_{90} value of MCF7 growth inhibition. This sufficient SCR-6852 in brain leads to efficiently shrink tumor cells growth and a significantly prolonged mice survival (100% animals survival treated with 10 mg/kg by the end of the study) in MCF-7 intracranial tumor model. Additionally, we observed that SCR-6852 not only accumulated in mice brain but also in rats, in dogs with a B/P ratio of 4, 7, and 15, respectively. SCR-6862 demonstrated consistent and high brain penetrability across multiple pre-clinical animal species, supporting it could penetrate well into human brain. Although the pre-clinical study [41] reported that the detectable Elacestrant in the intracranial tumor (the B/P ratio was about 0.6 according to reported data) which was most possibly less than anti-proliferation IC_{50} value, and the further efficacy study demonstrated only 43% animals survived to the end of the study at day 54. And up to now, there was no case with brain metastasis reported benefit from Elacestrant treatment in the clinic. The brain metastasis incidence of ER+/HER- breast cancer patients was 5~10% as reported in a previous study [42]. Since clinical studies had found that there existed some discordance for receptor phenotype between the primary tumor and systemic metastases. Kaidar-Person et al. [43] performed multi-institutional data analysis and revealed that the discordance rates for the expression of ER between the primary breast tumor and subsequent BM were 12% (for 20 patients in 167). In particular, 44 in 57 primary ER+ patients (77%) maintained the ER expression in BCBM. Overall, ER-target therapy was still needed and

meaningful for BCBM patients. SCR-6852 had higher brain exposures and consistent BBB penetration capability in preclinical species, supporting a high potential for clinical application in BCBM with ER-positive expression.

Endocrine therapy combined with CDK4/6 inhibitors is now the standard first-line treatment option for patients with HR+/HER2- mBC and may also be considered a standard option in the second-line setting, given the significant improvements in PFS and OS [44]. A phase III study investigated Fulvestrant plus Palbociclib in advanced HR+/HER2- breast cancer that had progressed on prior ET or recurred within 12 months of stopping adjuvant ET. Despite being heavily pretreated with ET, adding Palbociclib to Fulvestrant still more than doubled patients' PFS (11.2 vs. 4.6 months; HR=0.50 [95% CI=0.40–0.62], $P<0.0001$) and had prolonged OS by 10 months (median 39.7 vs. 29.7 months; HR=0.72 [95% CI=0.55–0.94]) [45]. In this study, the synergistic effects of SCR-6852 and Palbociclib were well demonstrated in anti-MCF7 growth in vitro and tumor inhibition in the MCF7 xenograft model. These results would support a combination therapy of SCR-6852 and CDK4/6 inhibitor in the clinical trial. Additionally, research revealed that tumor cells resistant to CDK4/6i could continue to rely on the ER pathway to drive tumor growth [46]. A clinical retrospective analysis demonstrated that hormonal therapy was effective, leading to significant PFS, in patients after Palbociclib progression [47]. The clinical benefits would be promising for SCR-6852 in CDK4/6 sensitive and resistant patients.

Conclusion

Based on structural optimization, we identified a novel SERD, SCR-6852. High potency and efficacy on ER degradation and cell growth inhibition of SCR-6852 were verified in multiple ER-positive cell lines with ESR wt or mutant. As an ER degrader, SCR-6852 exhibited a pure ER antagonistic efficacy on ER target genes expression and had no agonistic effects on endometrium that was different from SERM. In the xenograft model, oral administration of SCR-6852 demonstrated a relatively strong tumor growth inhibition with maximal TGI 123% (MCF7, 3, 10 mg/kg dosing). A combination of SCR-6852 and CDK4/CDK6 inhibitors revealed synergistically anti-tumor activities both in vitro and in vivo. Notably, SCR-6852 showed excellent brain penetration features of > 4 of a B/P ratio in multiple animal models. In an intracranial tumor model study, SCR-6852 concentrations in the brain were monitored at 419 ng/g (at 24 h for 7 days, 10 mg/kg dosing), which is much higher than the anti-proliferation IC_{90} value, and significantly

prolonged survival was finally observed with minimal tumor cell infiltration in the brain.

In summary, SCR-6852 is an oral SERD with high potency and efficacy on ER degradation and ER-positive breast cancer cells growth inhibition and excellent brain penetration of more than 4 B/P ratio in pre-clinical animal models making it an attractive candidate for intracranially-targeted therapeutic strategies involving advanced breast cancer patients even with brain metastases.

Abbreviations

ER	Estrogen receptor
ER+	Estrogen receptor positive
SERD	Selective estrogen receptor degrader or downregulator
ABC	Advanced breast cancer
BCBMs	Breast cancer brain metastases
ET	Endocrine therapy
AI	Aromatase inhibitors
SERM	Selective Estrogen Receptor Modulator
IC ₅₀ /IC ₉₀	The concentration of a drug or inhibitor needed to inhibit a biological process or response by 50% or 90%
DC ₅₀	The half-maximal degradation concentration that makes a protein for 50% degradation
Emax	The maximal effect at high drug concentrations when all the receptors are occupied by the drug
GREB1	Growth regulating estrogen receptor binding 1
AGR3	Anterior gradient 3, protein disulphide isomerase family member
ESR1	Estrogen receptor 1
CDK	Cyclin-dependent kinase
B/P	Brain-plasma ratio
PFS	Progression-free survival
OS	Overall survival
SOC	Standard of care

Supplementary Information

The online version contains supplementary material available at <https://doi.org/10.1186/s13058-023-01695-4>.

Additional file 1: Supporting docking figures and pharmacological data in vitro and in vivo.

Additional file 2: Target selectivity and transcription raw data.

Additional file 3: Raw data of WB gels.

Acknowledgements

This study was supported by the Nanjing Key Talent Project, Nanjing, China, and the State Key Laboratory of Translational Medicine and Innovative Drug Development, Nanjing, China.

Author contributions

Conceptualization, FZ and RT, designed the experiments, FZ, GY and LX; performed the drug design, PG and FT; molecular docking, JS; in vitro assays performance, GY, YL and JZ; in vivo studies and PK, LX, YG and LY; writing—original draft preparation, GY and LX; writing—review and editing, FZ and RT. All authors have read and agreed to the published version of the manuscript.

Funding

The Nanjing Key Talent Project, Nanjing, China.

Availability of data and materials

The datasets used and/or analyzed during the current study are available from the corresponding author on reasonable request.

Declarations

Ethics approval and consent to participate

The experimental protocol was approved and performed according to the guidelines of the State Council Regulations for Laboratory Animal Management (Enacted in 1988). Experiments in mice were approved by the Institutional Animal Care and Use Committee of the WuXi AppTec and Simcere, People's Republic of China.

Consent for publication

Not applicable.

Competing interests

The authors are the employees of Simcere Group.

Author details

¹State Key Laboratory of Neurology and Oncology Drug Development, Nanjing, China. ²Simcere Zaiming Pharmaceutical Co., Ltd., Shanghai, China. ³Jiangsu Simcere Pharmaceutical Co., Ltd., Nanjing, China.

Received: 26 April 2023 Accepted: 5 August 2023

Published online: 14 August 2023

References

- Ghoncheh M, Pournamdar Z, Salehiniya H. Incidence and mortality and epidemiology of breast cancer in the world. *Asian Pac J Cancer Prev*. 2016;17(S3):43–6.
- Lima SM, Kehm RD, Terry MB. Global breast cancer incidence and mortality trends by region, age-groups, and fertility patterns. *EClinicalMedicine*. 2021;38: 100985.
- Sung H, Ferlay J, Siegel RL, Laversanne M, Soerjomataram I, Jemal A, Bray F. Global cancer statistics 2020: GLOBOCAN estimates of incidence and mortality worldwide for 36 cancers in 185 countries. *CA Cancer J Clin*. 2021;71(3):209–49.
- Department of Defense Breast Cancer Research Program Breast Cancer Landscape2020. <https://cdmrp.health.mil/pubs/press/2021/21bcprpna> Accessed 19 Oct 2020.
- Hanker AB, Sudhan DR, Arteaga CL. Overcoming endocrine resistance in breast cancer. *Cancer Cell*. 2020;37(4):496–513.
- Lin NU, Winer EP. Advances in adjuvant endocrine therapy for postmenopausal women. *J Clin Oncol*. 2008;26(5):798–805.
- Burstein HJ. Systemic therapy for estrogen receptor-positive, HER2-negative breast cancer. *N Engl J Med*. 2020;383(26):2557–70.
- Reinert T, de Paula B, Shafae MN, Souza PH, Ellis MJ, Bines J. Endocrine therapy for ER-positive/HER2-negative metastatic breast cancer. *Chin Clin Oncol*. 2018;7(3):25.
- Jensen EV. On the mechanism of estrogen action. *Perspect Biol Med*. 1962;6(1):47–59.
- Bulut N, Altundag K. Does estrogen receptor determination affect prognosis in early stage breast cancers? *Int J Clin Exp Med*. 2015;8(11):21454.
- Ali S, Rasool M, Chaoudhry H, NP P, Jha P, Hafiz A, Mahfooz M, Abdus Sami G, Azhar Kamal M, Bashir S, et al. Molecular mechanisms and mode of tamoxifen resistance in breast cancer. *Bioinformation*. 2016;12(3):135–9.
- Lorizio W, Wu AH, Beattie MS, Rugo H, Tchu S, Kerlikowske K, Ziv E. Clinical and biomarker predictors of side effects from tamoxifen. *Breast Cancer Res Treat*. 2012;132(3):1107–18.
- Jeselsohn R, Yelensky R, Buchwalter G, Frampton G, Meric-Bernstam F, Gonzalez-Angulo AM, Ferrer-Lozano J, Perez-Fidalgo JA, Cristofanilli M, Gomez H. Emergence of constitutively active estrogen receptor- α mutations in pretreated advanced estrogen receptor-positive breast cancer. *ESR1-activating mutations in advanced breast cancer*. *Clin Cancer Res*. 2014;20(7):1757–67.
- Nathan MR, Schmid P. A review of fulvestrant in breast cancer. *Oncol Ther*. 2017;5(1):17–29.
- Rocca A, Maltoni R, Bravaccini S, Donati C, Andreis D. Clinical utility of fulvestrant in the treatment of breast cancer: a report on the emerging clinical evidence. *Cancer Manag Res*. 2018;10:3083–99.

16. Boer K. Fulvestrant in advanced breast cancer: evidence to date and place in therapy. *Ther Adv Med Oncol.* 2017;9(7):465–79.
17. Robertson JF, Bondarenko IM, Trishkina E, Dvorkin M, Panasci L, Manikhas A, Shparyk Y, Cardona-Huerta S, Cheung K-L, Philco-Salas MJ. Fulvestrant 500 mg versus anastrozole 1 mg for hormone receptor-positive advanced breast cancer (FALCON): an international, randomised, double-blind, phase 3 trial. *The Lancet.* 2016;388(10063):2997–3005.
18. Howell A, Robertson JF, Abram P, Lichinitser MR, Elledge R, Bajetta E, Watanabe T, Morris C, Webster A, Dimery I. Comparison of fulvestrant versus tamoxifen for the treatment of advanced breast cancer in postmenopausal women previously untreated with endocrine therapy: a multinational, double-blind, randomized trial. *J Clin Oncol.* 2004;22(9):1605–13.
19. Stemline Therapeutics Inc., a wholly owned subsidiary of Menarini Group, Receives Approval from U.S. FDA for ORSERDU™ (elacestrant) as the First and Only Treatment Specifically Indicated for Patients with ESR1 Mutations in ER+, HER2- Advanced or Metastatic Breast Cancer 2023. Radius Health, Inc. [<https://radiuspharm.com/stemline-therapeutics-inc-receives-approval-from-u-s-fda-for-orserdum-elacestrant-as-the-first-and-only-treatment-specifically-indicated-for-patients-with-esr1-mutations-in-er-her2-advanced-or/>] Accessed 30 Jan, 2023.
20. Bardia A, Kaklamani V, Wilks S, Weise A, Richards D, Harb W, Osborne C, Wesolowski R, Karuturi M, Conkling P, et al. Phase I study of elacestrant (RAD1901), a novel selective estrogen receptor degrader, in ER-positive, HER2-negative advanced breast cancer. *J Clin Oncol.* 2021;39(12):1360–70.
21. Hamilton EP, Oliveira M, Banerji U, Hernando C, Garcia-Corbacho J, Armstrong A, Ciruelos E, Patel MR, Incorvati J, Twelves C. A phase I dose escalation and expansion study of the next generation oral SERD AZD9833 in women with ER-positive, HER2-negative advanced breast cancer. *J Clin Oncol.* 2020;38(15_suppl):1024.
22. Lim E, Jhaveri KL, Perez-Fidalgo JA, Bellet M, Boni V, Perez Garcia JM, Estevez L, Bardia A, Turner NC, Villanueva R. A phase Ib study to evaluate the oral selective estrogen receptor degrader GDC-9545 alone or combined with palbociclib in metastatic ER-positive HER2-negative breast cancer. *J Clin Oncol.* 2020;38(15_suppl):1023.
23. Sun H, Xu J, Dai S, Ma Y, Sun T. Breast cancer brain metastasis: current evidence and future directions. *Cancer Med.* 2023;12(2):1007–24.
24. Zhang Y, Zhang TJ, Tu S, Zhang ZH, Meng FH. Identification of novel Src inhibitors: pharmacophore-based virtual screening, molecular docking and molecular dynamics simulations. *Molecules.* 2020;25(18):4094.
25. Corbeil CR, Williams CI, Labute P. Variability in docking success rates due to dataset preparation. *J Comput-Aided Mol Des.* 2012;26(6):775–86.
26. Bolger AM, Lohse M, Usadel B. Trimmomatic: a flexible trimmer for Illumina sequence data. *Bioinformatics.* 2014;30(15):2114–20.
27. Kim D, Langmead B, Salzberg SL. HISAT: a fast spliced aligner with low memory requirements. *Nat Methods.* 2015;12(4):357–60.
28. Roberts A, Trapnell C, Donaghey J, Rinn JL, Pachter L. Improving RNA-Seq expression estimates by correcting for fragment bias. *Genome Biol.* 2011;12(3):R22.
29. Trapnell C, Williams BA, Pertea G, Mortazavi A, Kwan G, van Baren MJ, Salzberg SL, Wold BJ, Pachter L. Transcript assembly and quantification by RNA-Seq reveals unannotated transcripts and isoform switching during cell differentiation. *Nat Biotechnol.* 2010;28(5):511–5.
30. Anders S, Pyl PT, Huber W. HTSeq—a Python framework to work with high-throughput sequencing data. *Bioinformatics.* 2015;31(2):166–9.
31. Diep CH, Ahrendt H, Lange CA. Progesterone induces progesterone receptor gene (PGR) expression via rapid activation of protein kinase pathways required for cooperative estrogen receptor alpha (ER) and progesterone receptor (PR) genomic action at ER/PR target genes. *Steroids.* 2016;114:48–58.
32. Love RR, Mazess RB, Barden HS, Epstein S, Newcomb PA, Jordan VC, Carbone PP, DeMets DL. Effects of tamoxifen on bone mineral density in postmenopausal women with breast cancer. *N Engl J Med.* 1992;326(13):852–6.
33. Love RR, Wiebe DA, Feys JM, Newcomb PA, Chappell RJ. Effects of tamoxifen on cardiovascular risk factors in postmenopausal women after 5 years of treatment. *J Natl Cancer Inst.* 1994;86(20):1534–9.
34. Kedar RP, Bourne TH, Powles TJ, Collins WP, Ashley SE, Cosgrove DO, Campbell S. Effects of tamoxifen on uterus and ovaries of postmenopausal women in a randomised breast cancer prevention trial. *Lancet.* 1994;343(8909):1318–21.
35. Awounfack CF, Zingué S, Koumabas B, Tueche AB, Tata CM, Tchuen-guem Fohouo F-N, Njamen D, Ndinteh DT. Ethanol-extracted Cameroonian propolis counteracts tamoxifen-induced endometrial hyperplasia by modulating apoptosis and proliferation-regulating proteins in the ovaries of intact wistar rats. 2022. *J Evidence-Based Complementary Altern Med.* <https://doi.org/10.1155/2022/2684742>.
36. Dustin D, Gu G, Fuqua SA. ESR1 mutations in breast cancer. *Cancer.* 2019;125(21):3714–28.
37. Jeselsohn R, Bergholz JS, Pun M, Cornwell M, Liu W, Nardone A, Xiao T, Li W, Qiu X, Buchwalter G, et al. Allele-specific chromatin recruitment and therapeutic vulnerabilities of ESR1 activating mutations. *Cancer Cell.* 2018;33(2):173–186 e5.
38. Raub TJ, Wishart GN, Kulanthaivel P, Staton BA, Ajamie RT, Sawada GA, Gelbert LM, Shannon HE, Sanchez-Martinez C, De Dios A. Brain exposure of two selective dual CDK4 and CDK6 inhibitors and the antitumor activity of CDK4 and CDK6 inhibition in combination with temozolomide in an intracranial glioblastoma xenograft. *Drug Metab Dispos.* 2015;43(9):1360–71.
39. De G, Zhang P, Buil L, iC H, Nishita T, Beijnen JH, Olaf VT. Buparlisib is a brain penetrable pan-PI3K inhibitor. *Sci Rep.* 2018;8(1):10784.
40. Shah N, Mohammad AS, Saralkar P, Sprowls SA, Vickers SD, John D, Tallman RM, Lucke-Wold BP, Jarrell KE, Pinti M, et al. Investigational chemotherapy and novel pharmacokinetic mechanisms for the treatment of breast cancer brain metastases. *Pharmacol Res.* 2018;132:47–68.
41. Garner F, Shomali M, Paquin D, Lyttle CR, Hattersley G. RAD1901: a novel, orally bioavailable selective estrogen receptor degrader that demonstrates antitumor activity in breast cancer xenograft models. *Anticancer Drugs.* 2015;26(9):948.
42. Kodack DP, Askoxylakis V, Ferraro GB, Fukumura D, Jain RK. Emerging strategies for treating brain metastases from breast cancer. *Cancer Cell.* 2015;27(2):163–75.
43. Kaidar-Person O, Meattini I, Jain P, Bult P, Simone N, Kindts I, Steffens R, Weltens C, Navarra P, Belkacemi Y. Discrepancies between biomarkers of primary breast cancer and subsequent brain metastases: an international multicenter study. *Breast Cancer Res Treat.* 2018;167(2):479–83.
44. Hui R, de Boer R, Lim E, Yeo B, Lynch J. CDK4/6 inhibitor plus endocrine therapy for hormone receptor-positive, HER2-negative metastatic breast cancer: The new standard of care. *Asia Pac J Clin Oncol.* 2021;17(Suppl 1):3–14.
45. Turner NC, Slamon DJ, Ro J, Bondarenko I, Im S-A, Masuda N, Colleoni M, DeMichele A, Loi S, Verma S. Overall survival with palbociclib and fulvestrant in advanced breast cancer. *N Engl J Med.* 2018;379(20):1926–36.
46. Patel HK, Tao N, Lee KM, Huerta M, Arlt H, Mullarkey T, Troy S, Arteaga CL, Bihani T. Elacestrant (RAD1901) exhibits anti-tumor activity in multiple ER+ breast cancer models resistant to CDK4/6 inhibitors. *Breast Cancer Res.* 2019;21(1):146.
47. Xi J, Oza A, Thomas S, Ademuyiwa F, Weilbaecher K, Suresh R, Bose R, Cherian M, Hernandez-Aya L, Frith A, et al. Retrospective analysis of treatment patterns and effectiveness of palbociclib and subsequent regimens in metastatic breast cancer. *J Natl Compr Canc Netw.* 2019;17(2):141–7.

Publisher's Note

Springer Nature remains neutral with regard to jurisdictional claims in published maps and institutional affiliations.